3D joint inversion of ground and airborne EM

C. Scholl[1], R. Mackie[1], W. Soyer[1], T. Kimura[1] and S. Hallinan[1]
[1]Viridien(Formerly CGG)
carsten.scholl@viridiengroup.com
randall.mackie@viridiengroup.com
wolfgang.soyer@viridiengroup.com
tom.kimura@viridiengroup.com
stephen.hallinan@viridiengroup.com

SUMMARY

The 3D multiphysics inversion modeling routines we have implemented cover most electromagnetic (EM) methods including passive and controlled-source methodologies; ground, airborne, and marine deployments; and include joint inversion options with gravity, magnetics, passive seismic tomography, and the use of geological constraints. We have now extended their capability to include 3D joint inversion of MT with controlled source frequency and time domain airborne electromagnetics (AEM).

Keywords: 3D, inversion, joint, airborne, MT

INTRODUCTION

Mineral exploration is increasingly targeting more complex prospects, e.g. below overburden, in heterogeneous host rocks, and at greater depths. Reliable resistivity imaging in these situations requires deep-looking methods like magnetotellurics (MT) in addition to the densely sampled but nearer-surface airborne electromagnetics (AEM), and full 3D modeling to correctly account for the geology.

In the past years we implemented different 3D inversion modeling routines for EM and other data. One package, RLM-3D, focusses on MT and other frequency domain methods (Mackie and Watts, 2012; Mackie et al., 2023; Soyer et al., 2021), while the other (Otze) deals with most active source methods, which includes frequency and time domain active AEM (Scholl and Sinkevic, 2012; Scholl and Miorelli, 2019; Scholl et al., 2024).

We have now combined the two codes to carry out simultaneous joint inversions, for example of MT and AEM data. This extended joint EM inversion capability also includes ground loop TEM, ground controlled source EM (CSAMT/CSEM) and passive airborne EM (AFMAG). Integration of geological data in the 3D inversions (faults, overburden horizons, dip and strike, etc.) is available as previously.

METHOD

Both inversion codes are modular, so it was relatively straightforward to mix and match the required tasks of different methods to create a joint inversion code.

RLM-3D works on structured, rectangular grids. Otze allows for more flexible, unstructured grids (Scholl and Miorelli, 2019). It was therefore decided to use the inversion core of RLM-3D and call Otze modules to compute synthetics and data gradients for the data types that RLM-3D does not natively support.

Examples

The example in Figure 1 is from a project where both ground MT and AEM, specifically from a time domain system (HELITEM) were available. All sections shown in the Figure are fence sections through 3D inversion results.

The uppermost panel shows the result of the HELITEM single domain result with the deeper parts that are poorly resolved removed. This result was generated with Otze.

The second panel from the top shows an MT-only inversion result, derived using RLM-3D. Overall, the model appears smoother in the near surface.

EMIW2024 abstracts are distributed under the Creative Commons Attribution 4.0 Unported License.
Authors retain the copyright of the abstract but grant any third party the right to use the abstract freely as long as its original authors and citation details are identified.
To view a copy of this license, visit https://creativecommons.org/licenses/by/4.0/

Differences to the HELITEM result are mostly due to the lower lateral resolution of the much sparser MT sites compared with the HELITEM data set. It should be noted that Otze and RLM-3D by default use a different smoothness criterion: While RLM-3D minimizes the curvature of the resistivities, Otze minimizes their gradients. These data however, provide a better definition of the features at depth.

The two lower panels show results of the joint inversion of both data sets. We found that when inverting both data sets simultaneously, several tests with different data weightings between the data sets were required. To do these efficiently, we initially ran the 3D inversions with a mixed approach where the MT forwards were done with the full 3D forward algorithm, while the computationally more expensive AEM simulations were done with a 2.5D forward approach (Scholl et al., 2024). The best result of these runs is shown in the third panel.

This model was subsequently used as a starting point for a full 3D joint inversion. The result is shown in the bottom panel. It exhibits minor differences to the result obtained with the mixed dimensionality approach.

Comparing the single domain to the joint inversions, the AEM section (top panel) exhibits high resolution in the near surface, whereas the MT section (second panel) shows better defined features at depth. The joint inversion section (third and bottom panel) shows combined features of two methods, the near surface from AEM and more from MT in deeper depth.

The second panel shows a small conductive feature in the near surface that correlates with mineralization that was present when the MT data were collected in 1996-1999, but that was subsequently mined before the AEM survey of 2022, and is not present in the AEM inversion. Additional infrastructure like roads and buildings were also added during the mining phase and were not present when the earlier dataset was collected. These changes over time must be taken into account when jointly interpreting datasets that span a significant time period with potential differences in the resistivity and geological structure. The HELITEM data were edited over the areas that saw recent development.

However, for this project we decided not to mask out any part of data where the geological change has occurred, and the joint inversion kept the majority of low resistive zones visible in two different methods.

The central parts of this profile show a shallow conductive feature that is imaged in all inversions involving the HELITEM data but is completely missing in the MT-only result. Currently, it is not clear if this feature was missed by MT due to the site spacing or if it is due to recently added infrastructure.

References

Mackie, R.L., and Watts, M.D., 2012, Detectability of 3-D sulphide targets with AFMAG: SEG Technical Program Expanded Abstracts, 1-4.

Mackie, R.L., Soyer, W., Hallinan, S., and Godsmark, B., 2023, Complete earth 3D modelling of land controlled-source EM: 4th AEGC Geoscience Convention, Brisbane.

Soyer, W., Mackie, R.L., Hallinan, S., Miorelli, F., Pavesi, A., Garanzini, S., Sagala, B., and Siagan, H., 2021, Geophysics over high enthalpy fields: lessons from RLM-3D magnetotelluric and joint inversions: Proceedings World Geothermal Congress, Reykjavik

Scholl, C. and Sinkevich, V.A., 2012, Modeling mCSEM data with a finite difference approach and an unstructured model grid in the presence of bathymetry: 21st EM Induction Workshop, Darwin, Australia.

Scholl, C. and Miorelli, F., 2019, Airborne EM inversion on vertically unstructured model grids: Exploration Geophysics, DOI: 10.1080/08123985.2019.1668239.

Scholl, C., Kimura, T., and Hallinan, S., 2024, 3D airborne EM inversion with 1D, 2D and 3D forward solvers: KEGS Symposium, Toronto.

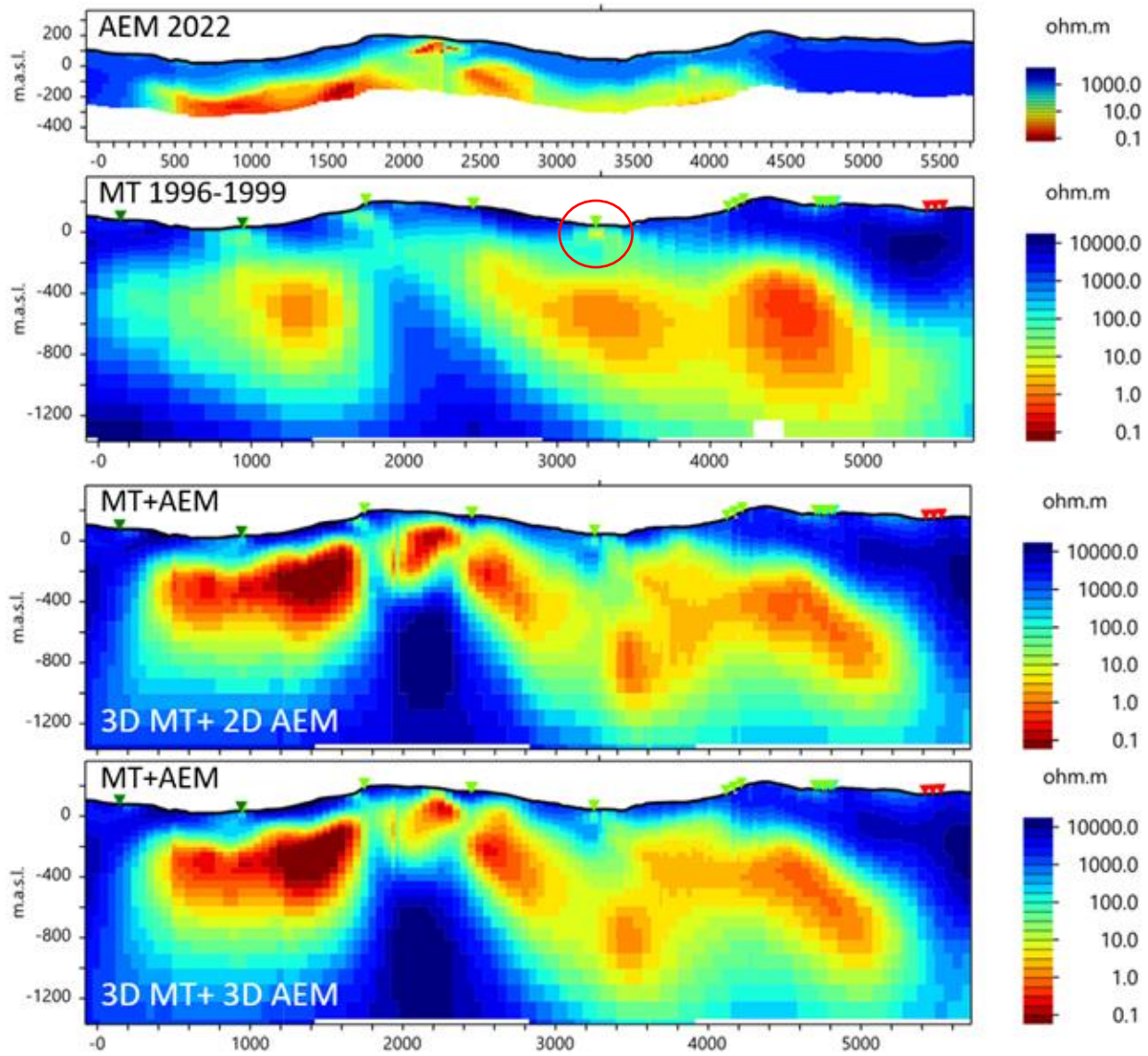

Figure 1. Fence sections through 3D inversion models: AEM inversion (top), MT (second), Joint MT and AEM inversion result (third and bottom). The triangles mark the position of MT sites. The AEM data are roughly perpendicular to the section with a line spacing of 100 m. Shallow discrepancies relate to presence of infrastructure (absent before 1999) and mineralized rock (mined in 2022, red circle in the second panel)

EMIW2024 abstracts are distributed under the Creative Commons Attribution 4.0 Unported License.
Authors retain the copyright of the abstract but grant any third party the right to use the abstract freely as long as its original authors and citation details are identified.
To view a copy of this license, visit https://creativecommons.org/licenses/by/4.0/